ELSEVIER

J. Non-Newtonian Fluid Mech. 144 (2007) 30–41

Journal of Non-Newtonian Fluid Mechanics

www.elsevier.com/locate/jnnfm

Global stability of equilibrium manifolds, and "peaking" behavior in quadratic differential systems related to viscoelastic models

Raanan Fattal [a], Ole H. Hald [a], Guy Katriel [b], Raz Kupferman [b,*]

[a] *Department of Mathematics, University of California, Berkeley, CA 94720, United States*
[b] *Institute of Mathematics, The Hebrew University, Jerusalem 91904, Israel*

Received 18 September 2006; received in revised form 31 January 2007; accepted 12 March 2007

Abstract

We study a model inspired by the Oldroyd-B equations for viscoelastic fluids. The objective is to better understand the nonlinear coupling between the stress and velocity fields in viscoelastic flows, and thus gain insight into the reasons that cause the loss of accuracy of numerical computations at high Weissenberg number. We derive a model system by discarding the stress-advection and stress-relaxation terms in the Oldroyd-B model. The reduced (unphysical) model, which bears some resemblance to a viscoelastic solid, only retains the stretching of the stress due to velocity gradients and the induction of velocity by the stress field. Our conjecture is that such a system always evolves toward an equilibrium in which the stress builds up such to cancel the external forces. This conjecture is supported by numerous simulations. We then turn our attention to a finite dimensional model (i.e., a set of ordinary differential equations) that has the same algebraic structure as our model system. Numerical simulations indicate that the finite-dimensional analog has a globally attracting equilibrium manifold. In particular, it is found that subsets of the equilibrium manifold may be unstable, leading to a "peaking" behavior, where trajectories are repelled from the equilibrium manifold at one point, and are eventually attracted to a stable equilibrium point on the same manifold. Generalizations and implications to solutions of the Oldroyd-B model are discussed.

Keywords: Oldroyd-B model; Equilibrium manifold; Global stability; Nonlinear analysis

1. Introduction

The Oldroyd-B model for viscoelastic fluids in the creeping flow regime consists of a constitutive equation,

$$\frac{\partial \boldsymbol{c}}{\partial t} + (\boldsymbol{u}\cdot\nabla)\boldsymbol{c} = (\nabla \boldsymbol{u})^{\mathrm{T}}\cdot\boldsymbol{c} + \boldsymbol{c}\cdot(\nabla\boldsymbol{u}) - \frac{1}{\lambda}(\boldsymbol{c}-I) \tag{1.1}$$

coupled to a Stokes system,

$$-\nabla p + \nu_{\mathrm{s}}\Delta\boldsymbol{u} + G\,\mathrm{div}\,\boldsymbol{c} + \boldsymbol{f} = 0, \quad \mathrm{div}\,\boldsymbol{u} = 0. \tag{1.2}$$

Here $\boldsymbol{u} = \boldsymbol{u}(\boldsymbol{x}, t)$ is the velocity vector field, $p = p(\boldsymbol{x}, t)$ is the scalar pressure field, $\boldsymbol{c} = \boldsymbol{c}(\boldsymbol{x}, t)$ is the (symmetric positive-definite) conformation tensor with $(\mathrm{div}\,\boldsymbol{c})_i = \sum_j \partial c_{ji}/\partial x_j$, ν_{s} is the solvent viscosity, G the elastic modulus, λ the polymeric relaxation time, and $\boldsymbol{f} = \boldsymbol{f}(\boldsymbol{x})$ is a force field. The constitutive Eq. (1.1) describes the evolution of the conformation tensor as a composition of advection, deformation, and relaxation. The flow field, which governs the advection and the deformation is induced by the conformation tensor through the Stokes system (1.2), thus constituting a nonlinear feedback mechanism (see [1,2] for a presentation of various constitutive models).

Our primary motivation is to better understand the interplay between the various terms in this system, with the dual goals of (i) progressing toward the development of an existence theory, and (ii) gain insight into the reasons that make numerical computations lose accuracy at modestly large Weissenberg numbers. A strategy that often yields useful information in complex dynamics of this sort is the analysis of "toy models" that focus on certain terms in the equations while discarding all other. For example, by focusing the attention on the balance between stress-advection and stress-deformation, two of the co-authors identified a numerical instability responsible for blowup at high Weissenberg numbers [3–5]. Although this instability can be remedied by a simple change of variables (the log-c formulation), computations still exhibit a frustrating loss

* Corresponding author. Tel.: +972 2 658 4159; fax: +972 2 563 0702.
E-mail addresses: raananf@gmail.com (R. Fattal), hald@math.berkeley.edu (O.H. Hald), haggaik@wowmail.com (G. Katriel), raz@math.huji.ac.il (R. Kupferman).

0377-0257/$ – see front matter © 2007 Elsevier B.V. All rights reserved.
doi:10.1016/j.jnnfm.2007.03.003

of accuracy in regions of large stress, whose reasons are not yet understood.

Sticking to the same strategy, we investigate here the nonlinear feedback mechanism between the stress-induced velocity and the stress-buildup due to deformation. Specifically, we first discard stress-relaxation by letting $\lambda \to 0$, while retaining the elastic modulus G fixed, thus letting the polymeric viscosity $\nu_p = G\lambda$ tend to infinity as well. This transforms the model into that of an incompressible viscoelastic solid with modulus G and retardation time ν_s/G (the so-called Kelvin–Voigt model). We then discard stress-advection, remaining with an (unphysical) model in which the conformation tensor is stretched and rotated by the flow field, the latter being induced by the conformation tensor through the Stokes system:

$$\frac{\partial \boldsymbol{c}}{\partial t} = (\nabla \boldsymbol{u})^{\mathrm{T}} \cdot \boldsymbol{c} + \boldsymbol{c} \cdot (\nabla \boldsymbol{u}),$$
$$-\nabla p + \Delta \boldsymbol{u} + \operatorname{div} \boldsymbol{c} + \boldsymbol{f} = 0, \quad \operatorname{div} \boldsymbol{u} = 0 \tag{1.3}$$

(the retardation time has been set to 1). For concreteness we consider the simplest geometry, $\Omega = \mathbb{T}^2$, a two-dimensional fluid in a doubly periodic box (i.e., on a torus), which obviates the need for boundary conditions.

Further motivation for studying a model of the form (1.3) is now given. In the creeping flow regime, i.e., in the absence of inertia, the flow field is determined instantaneously by the stress field. In analogy to the motion generated by a mechanical spring, we expect this induced flow to relax the stress. Consider momentarily a system without external forces, $\boldsymbol{f} = 0$. The Stokes system can then be represented as an equivalent variational problem,

$$\boldsymbol{u} = \underset{\boldsymbol{u}}{\operatorname{argmin}} \|\nabla \boldsymbol{u} + \boldsymbol{c}\|_2 \quad \text{such that} \quad \operatorname{div} \boldsymbol{u} = 0, \tag{1.4}$$

where the norm $\|\cdot\|_2$ is the L^2 Frobenius norm. That is, the velocity gradient is the best L^2 approximation to $(-\boldsymbol{c})$ taken among all divergence-free flow fields. Proceeding heuristically, if indeed $\nabla \boldsymbol{u} \approx -\boldsymbol{c}$ (keeping in mind that $\boldsymbol{c}$ is symmetric), the constitutive Eq. (1.1) is approximated by

$$\frac{\partial \boldsymbol{c}}{\partial t} + (\boldsymbol{u} \cdot \nabla)\boldsymbol{c} \approx -2\boldsymbol{c}^2 - \frac{\nu_p}{\lambda}(\boldsymbol{c} - I). \tag{1.5}$$

Since the stress is positive definite, such dynamics represent a negative feedback capable of eradicating large stresses. It is such a stress relaxation mechanism that we are trying to better understand. To simplify the analysis we isolate this mechanism, discarding stress-advection and stress-relaxation.

Note that had the stress lost its positive-definiteness (as might happen in numerical calculations), this feedback mechanism would have become positive, leading to blowup in *finite time*. This observation agrees with numerical experiments. In [6] loss of convergence and blowup has been reported to occur after a loss of positivity. On the other hand, schemes which impose the positive-definiteness of the stress are known to be much more robust (e.g., Brownian configuration fields [7]).

We now revert our attention to the model system (1.3). Without loss of generality, we may express the force field as the divergence of a stress field, $\boldsymbol{f}(\boldsymbol{x}) = -\operatorname{div} \boldsymbol{a}(\boldsymbol{x})$ (the choice of $\boldsymbol{a}(\boldsymbol{x})$ is non-unique), so that the Stokes system takes the form

$$-\nabla p + \Delta \boldsymbol{u} = \operatorname{div}(\boldsymbol{a} - \boldsymbol{c}), \quad \nabla \cdot \boldsymbol{u} = 0. \tag{1.6}$$

Let $\nabla^\perp := (\partial/\partial y, -\partial/\partial x)^{\mathrm{T}}$ be the orthogonal gradient operator; it maps scalar fields into vector fields. Its adjoint $-\operatorname{div}^\perp := (-\nabla^\perp \cdot)$, the orthogonal divergence, maps vector fields into scalar fields. Applying the orthogonal divergence operator on (1.6) and expressing the divergence-free flow field as the orthogonal gradient of a stream function, $\boldsymbol{u} = \nabla^\perp \psi$, we obtain a bi-harmonic equation for the stream function,

$$\Delta^2 \psi = \operatorname{div}^\perp \operatorname{div}(\boldsymbol{a} - \boldsymbol{c}).$$

The bi-harmonic operator on a torus in not invertible (its inverse Δ^{-2} is not uniquely defined), however it is only the velocity gradient that enters into the model system (1.3), and the latter is well-defined by the zero-degree integro-differential operator,

$$\nabla \boldsymbol{u} = \nabla \nabla^\perp \Delta^{-2} \operatorname{div}^\perp \operatorname{div}(\boldsymbol{a} - \boldsymbol{c}) =: \mathcal{P}(\boldsymbol{a} - \boldsymbol{c}). \tag{1.7}$$

Thus, (1.3) can be written as a closed (non-local) equation for the conformation field $\boldsymbol{c}(\boldsymbol{x}, t)$,

$$\frac{\partial \boldsymbol{c}}{\partial t} = \mathcal{P}^{\mathrm{T}}(\boldsymbol{a} - \boldsymbol{c}) \cdot \boldsymbol{c} + \boldsymbol{c} \cdot \mathcal{P}(\boldsymbol{a} - \boldsymbol{c}), \tag{1.8}$$

where we have introduced the short-hand notation for matrix transpose, $[\mathcal{P}^{\mathrm{T}}(\boldsymbol{c})](\boldsymbol{x}) := [\mathcal{P}(\boldsymbol{c})(\boldsymbol{x})]^{\mathrm{T}}$.

If we endow the space of tensor fields over Ω with the standard inner-product,

$$(\boldsymbol{c}_1, \boldsymbol{c}_2) := \int_\Omega \operatorname{tr}[\boldsymbol{c}_1^{\mathrm{T}}(\boldsymbol{x}) \cdot \boldsymbol{c}_2(\boldsymbol{x})]\, \mathrm{d}\boldsymbol{x}, \tag{1.9}$$

then it is easy to verify that the operator $\mathcal{P}$ defined by (1.7) satisfies the following properties: (i) It is a linear operator. (ii) It is symmetric with respect to the inner-product (1.9). (iii) It is a projection, $\mathcal{P} \circ \mathcal{P} = \mathcal{P}$, in fact, an orthogonal projection. (iv) Its range consists of traceless tensor fields, $\operatorname{tr} \mathcal{P}(\boldsymbol{c}) = 0$. (v) The ranges of $\mathcal{P}$ and $\mathcal{P}^{\mathrm{T}}$ are orthogonal; for every pair of tensor fields $\boldsymbol{c}_1, \boldsymbol{c}_2$,

$$(\mathcal{P}^{\mathrm{T}}(\boldsymbol{c}_1), \mathcal{P}(\boldsymbol{c}_2)) = 0.$$

Additional properties of $\mathcal{P}$ can be inferred from these five properties, but we defer this to the next section. It should be noted that the algebraic properties satisfied by $\mathcal{P}$ do not depend on the geometry of the system; the same would hold in the whole plane, or for a bounded geometry with suitable boundary conditions.

Eq. (1.8) has a very suggestive form. Viewed as a matrix linear equation for $\boldsymbol{c}$ with time-dependent amplification matrix $\mathcal{P}(\boldsymbol{a} - \boldsymbol{c})$, the amplification matrix is, in a certain sense, anti-linear to $\boldsymbol{c}$ ($\mathcal{P}$ is a positive operator), i.e., there seems to be a stabilizing negative feedback. In fact, (1.8) is reminiscent of a Ricatti equation in which the quadratic term has a negative coefficient; under such conditions it is well known that positive initial data yield a solution which, as $t \to \infty$, tends to an equilibrium solution (a fixed point).

These heuristic considerations have led us to the following speculation:

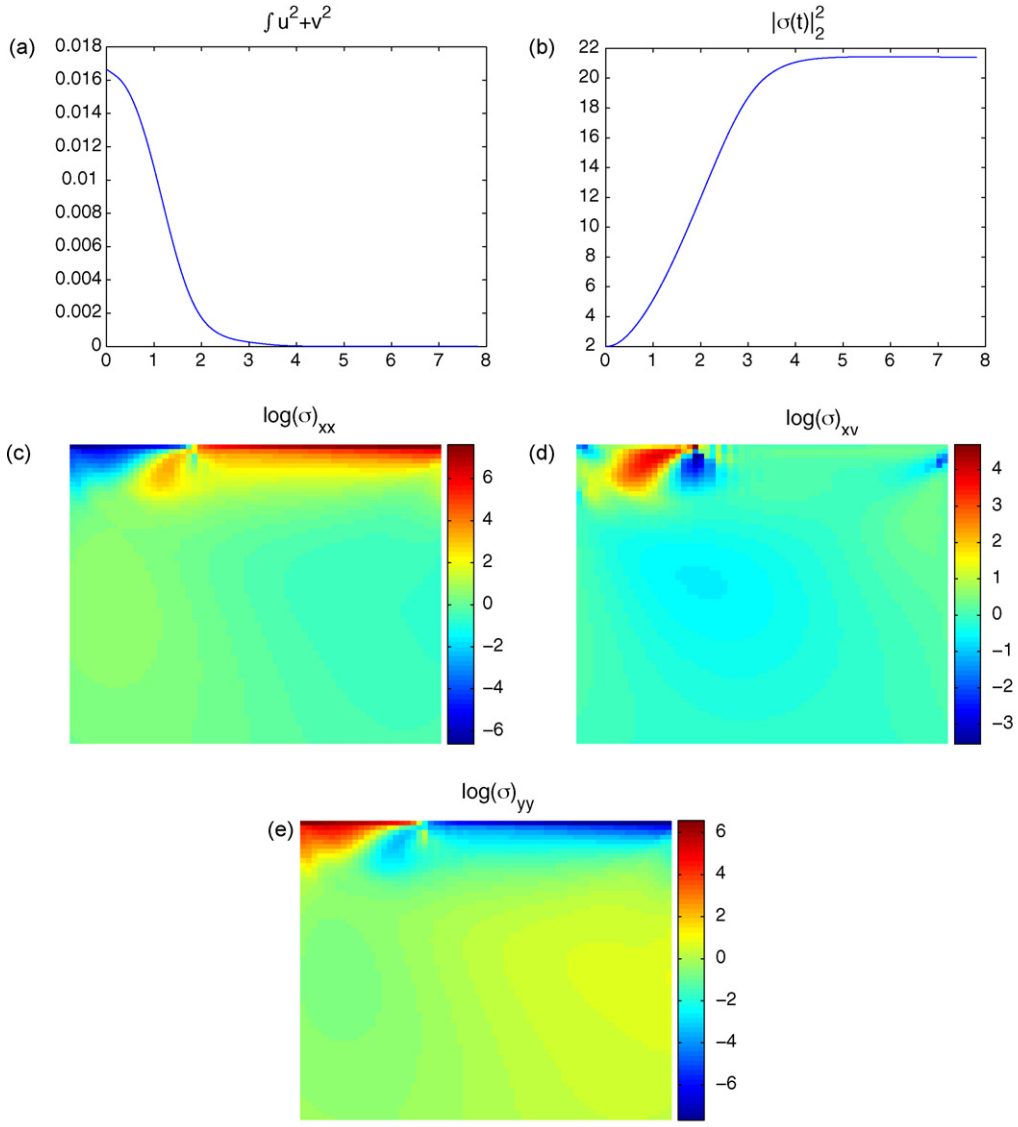

Fig. 1. Simulation results of system (1.3) for a lid-driven cavity geometry; the upper wall moves to the left with velocity $\boldsymbol{u}(x, 1) = -1$. The initial conditions are $\boldsymbol{c}(\boldsymbol{x}) = \boldsymbol{I}$. (a) Time evolution of the L^2 norm of the velocity, which decays to zero exponentially fast. (b) Time evolution of the L^2-norm of the stress. (c–e) Steady-state profiles of the *xx*, *xy*, and *yy*-components of $\log \boldsymbol{c}$.

Let $\boldsymbol{c}(\boldsymbol{x}, t)$ be a solution of (1.8) with symmetric positive-definite initial data $\boldsymbol{c}_0(\boldsymbol{x}) = \boldsymbol{c}(\boldsymbol{x}, 0)$, then $\boldsymbol{c}(x, t)$ converges, as $t \to \infty$, to an equilibrium solution of the system.

By "equilibrium" we mean a state of stress that counters the external forces (whether these are bulk forces or boundary forces), thus causing the velocity to vanish. Since our model is closely related to that of a viscoelastic solid (up to the artificial omission of the advection term), our conjecture can be understood in physical terms: a solid cannot be stretched indefinitely by a constant force. These considerations hold for systems driven by forcing; shearing boundary conditions can also be cast in such category. On the other hand, we do not expect it to remain correct in situations where (non-trivial) boundary conditions are prescribed for normal components of the flow field.

We have tested this conjecture numerically, and found that indeed, for all choices of inhomogeneous stress fields $\boldsymbol{a}(\boldsymbol{x})$ and (symmetric positive-definite) initial data $\boldsymbol{c}_0(\boldsymbol{x})$, the solution tends to a steady-state $\boldsymbol{c}^*(\boldsymbol{x})$, which lies on the equilibrium manifold, $\mathcal{P}(\boldsymbol{a} - \boldsymbol{c}^*) = 0$.

The convergence of the stress to a static equilibrium was found to be extremely robust, even in the presence of singular geometries. In Fig. 1 we show simulation results for a lid-driven cavity geometry. The flow takes place in a unit square, with the upper boundary moving to the left with velocity $\boldsymbol{u}(x, 1) = -1$. As shown in the figure, a strong stress profile forms near the moving boundary until, eventually, the velocity field within the cell vanishes. Thus, the system generates a delta-sheet-like stress field, which "shields" the interior of the cell from the singular forces induced by the discontinuous boundary conditions. The same phenomenon repeats in Fig. 2 for a planar 4:1 contracting

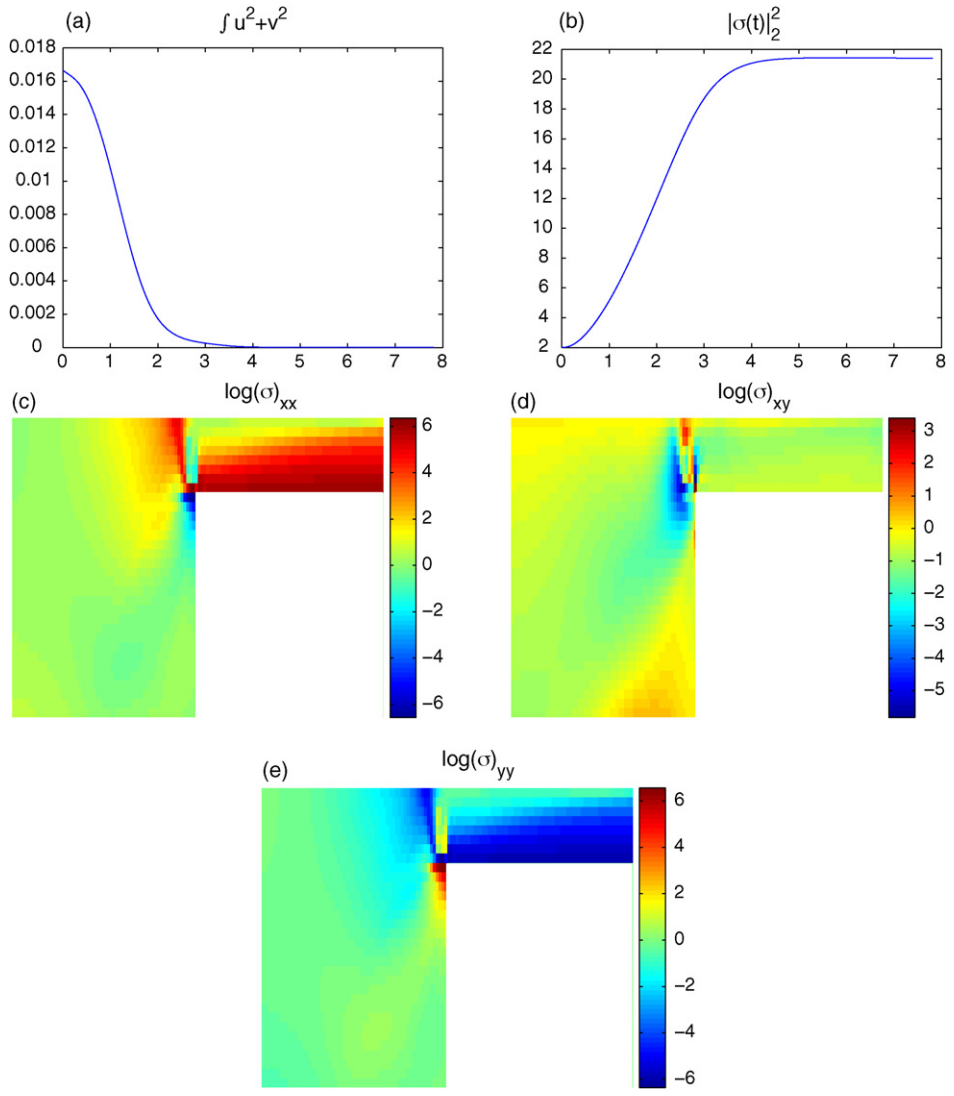

Fig. 2. (a–e) Simulation results of system (1.3) for a 4:1 contraction channel, with the fluid forced by a constant pressure gradient. See the caption of Fig. 1 for details.

channel, where the fluid is pushed into the system by a fixed pressure gradient. As pointed out above, we only consider systems driven by constant forces; no such equilibrium is expected to form if, instead, the fluid is pushed into the channel at constant flow rate. Here, strong stresses are generated at the contraction inlet, canceling eventually the flow induced by the pressure gradient. It should be emphasized, however, that in both cases, the results do not converge upon mesh refinement, at least not in any standard sense. These simulations are not supposed to reproduce any physical reality. They only serve as a demonstration of the robustness of the negative-feedback mechanism inherent in the velocity–stress coupling.

All our attempt to prove the validity of the above conjecture have so far failed; a detailed account of partial results will be presented in the next section. Yet, the understanding of the globally stabilizing mechanism of the dynamics (1.8) seems crucial for the understanding of the nonlinear feedback mechanism in viscoelastic models. In particular, it is of fundamental importance to understand which properties of this dynamical system should be retained in finite-dimensional approximations, to preserve the stabilizing mechanism.

With this in mind, we constructed a family of finite-dimensional dynamical systems (i.e., ordinary differential systems), which carry a structure similar to that of (1.8). This class of toy models is presented in Section 3. The finite-dimensional toy model is much easier to manipulate, and the global stability of its equilibrium manifold – which is a hyper-plane – is unambiguously defined. Numerical simulations indicate that the equilibrium manifold is indeed globally attracting for positive initial data, yet, despite the much simpler structure of the system, we were still unable to prove global stability. In this respect, the reduction to finite dimension does not simplify the analysis of the stability mechanism.

Most methods for proving the global asymptotic stability of equilibrium points, or equilibrium manifolds are based, in a way or another, on the construction of Lyapunov functions; one finds a function of the state space that is on the one hand bounded from below, and on the other hand decreases monotonically along tra-

jectories. Thus, the Lyapunov function tends to a limit as $t \to \infty$, and asymptotic convergence to the equilibrium manifold usually follows. An examination of particular examples in the present problem clarifies why all such methods are bound to fail. The equilibrium manifold may have subsets that are linearly unstable. Solutions that are initially in the vicinity of these unstable regions are exponentially repelled from the equilibrium manifold, before being eventually attracted to a stable equilibrium point. In others words, there exists a continuum of heteroclinic orbits connecting the equilibrium manifold to itself. These findings are indicative of a very non-common stability mechanism, which, we believe, is intrinsic to many models for viscoelastic fluids.

2. Preliminary analysis

Throughout this section it is assumed that the external stress field $\boldsymbol{a}(\boldsymbol{x})$ and the (symmetric positive-definite) initial conditions $\boldsymbol{c}_0(\boldsymbol{x})$ are sufficiently regular, such that a unique solution $\boldsymbol{c}(\boldsymbol{x}, t)$ exists for all positive times. Whether such an assumption is justified is not known, and its analysis seems as complex as the analysis of the Oldroyd-B model. It should only be pointed out that the natural space in which solutions should be sought is $L^{\infty,+}$, the cone of bounded symmetric positive-definite tensor fields.

First, we show that the positive-definiteness of $\boldsymbol{c}(\boldsymbol{x}, t)$ is guaranteed for all times.

Proposition 2.1. *The scalar-valued function* $\det \boldsymbol{c}(\boldsymbol{x}, t)$ *is conserved by the dynamics* (1.8).

Proof. This is an immediate consequence of the fact that the range of $\mathcal{P}$ consists of traceless tensor fields (equivalently, that the flow field is divergence-free),

$$\frac{\partial}{\partial t}\log\,\det \boldsymbol{c} = \operatorname{tr}\left(\boldsymbol{c}^{-1}\cdot\frac{\partial \boldsymbol{c}}{\partial t}\right) = \operatorname{tr}\mathcal{P}^{\mathrm{T}}(\boldsymbol{a}-\boldsymbol{c}) + \operatorname{tr}\mathcal{P}(\boldsymbol{a}-\boldsymbol{c}) = 0. \quad \square$$

Corollary 2.1. *The tensor field* $\boldsymbol{c}(\boldsymbol{x}, t)$ *remains symmetric positive-definite for all* $t \geq 0$.

Proof. Symmetry follows from the structure of the equations. Positivity follows from the conservation of the determinant, as it implies that none of the eigenvalues of $\boldsymbol{c}(\boldsymbol{x}, t)$ can vanish, and by continuity cannot change sign. $\square$

Our goal is to show that the equilibrium manifold,

$$\mathcal{M} = \{\boldsymbol{c} \in L^{\infty,+} : \mathcal{P}(\boldsymbol{a}-\boldsymbol{c}) = 0\}$$

is globally attracting for $\boldsymbol{c}_0 \in L^{\infty,+}$. A necessary condition for this to hold is that (1.8) does not have other equilibria within $L^{\infty,+}$. This is guaranteed by the following proposition.

Proposition 2.2. *The set of fixed points for* (1.8) *in* $L^{\infty,+}$ *coincides with the manifold* $\mathcal{M}$.

Proof. Note that

$$\frac{\partial \boldsymbol{c}^{-1}}{\partial t} = -\boldsymbol{c}^{-1}\cdot\mathcal{P}^{\mathrm{T}}(\boldsymbol{a}-\boldsymbol{c}) - \mathcal{P}(\boldsymbol{a}-\boldsymbol{c})\cdot\boldsymbol{c}^{-1},$$

hence, using the orthogonality of the ranges of $\mathcal{P}$ and $\mathcal{P}^{\mathrm{T}}$,

$$\left(\frac{\partial \boldsymbol{c}}{\partial t}, \frac{\partial \boldsymbol{c}^{-1}}{\partial t}\right) = -2\|\boldsymbol{c}^{1/2}\cdot\mathcal{P}(\boldsymbol{a}-\boldsymbol{c})\cdot\boldsymbol{c}^{-1/2}\|_2^2 \leq 0,$$

with equality if and only if $\mathcal{P}(\boldsymbol{a}-\boldsymbol{c}) = 0$. That is, $\partial \boldsymbol{c}/\partial t = 0$ if and only if $\boldsymbol{c} \in \mathcal{M}$. $\square$

Most methods for proving that an equilibrium point, or an equilibrium manifold are attracting, are based on the construction of a suitable Lyapunov functional. A natural candidate for such a functional is the square of the L^2-distance from the equilibrium manifold,

$$V[\boldsymbol{c}(\cdot)] = (\mathcal{P}(\boldsymbol{a}-\boldsymbol{c}), \mathcal{P}(\boldsymbol{a}-\boldsymbol{c})).$$

Differentiating V along trajectories of (1.8), using the self-adjointness and idempotence of $\mathcal{P}$, we get

$$\begin{aligned}\frac{\mathrm{d}}{\mathrm{d}t}V[\boldsymbol{c}(\cdot,t)] &= -2(\mathcal{P}(\boldsymbol{a}-\boldsymbol{c}), \mathcal{P}^{\mathrm{T}}(\boldsymbol{a}-\boldsymbol{c})\cdot\boldsymbol{c} + \boldsymbol{c}\cdot\mathcal{P}(\boldsymbol{a}-\boldsymbol{c})) \\ &= -2\|\boldsymbol{c}^{1/2}\cdot\mathcal{P}(\boldsymbol{a}-\boldsymbol{c})\|_2^2 \\ &\quad +2\int_\Omega \det\mathcal{P}(\boldsymbol{a}-\boldsymbol{c})\operatorname{tr}\boldsymbol{c}\,\mathrm{d}\boldsymbol{x}.\end{aligned}$$

It is easy to construct pairs $\boldsymbol{a}$, $\boldsymbol{c}$ for which the right-hand side it positive, thus excluding V as a Lyapunov functional. Various attempts to construct Lyapunov functionals of either "energy type" or "entropy type" (see [8]) have failed similarly, raising the doubt whether the dynamics (1.8) are at all dissipative.

Since the determinant of $\boldsymbol{c}(\boldsymbol{x}, t)$ is preserved, its trace is bounded from below by

$$\operatorname{tr}\boldsymbol{c}(\boldsymbol{x}, t) \geq 2\sqrt{\det\boldsymbol{c}(\boldsymbol{x}, t)} = 2\sqrt{\det\boldsymbol{c}_0(\boldsymbol{x})}.$$

Consider the evolution of the integral of $\operatorname{tr}\boldsymbol{c}$,

$$\begin{aligned}\frac{\mathrm{d}}{\mathrm{d}t}\int_\Omega \operatorname{tr}\boldsymbol{c}\,\mathrm{d}\boldsymbol{x} &= 2(\boldsymbol{c}, \mathcal{P}(\boldsymbol{a}-\boldsymbol{c})) \\ &= \|\mathcal{P}(\boldsymbol{a})\|_2^2 - \|\mathcal{P}(\boldsymbol{c})\|_2^2 - \|\mathcal{P}(\boldsymbol{a}-\boldsymbol{c})\|_2^2.\end{aligned}$$

An immediate conclusion is that the integral over the trace of $\boldsymbol{c}(\boldsymbol{x}, t)$, which can be used as a norm on the space of positive-definite tensor fields, has at most a linear growth rate,

$$\frac{\mathrm{d}}{\mathrm{d}t}\int_\Omega \operatorname{tr}\boldsymbol{c}\,\mathrm{d}\boldsymbol{x} \leq \|\mathcal{P}(\boldsymbol{a})\|_2^2.$$

In particular, if $\mathcal{P}(\boldsymbol{a}) = 0$, i.e., in the absence of external forcing, this norm is monotonically decreasing and $\boldsymbol{c}(\boldsymbol{x}, t)$ must approach the equilibrium manifold $\mathcal{P}(\boldsymbol{c}) = 0$. In the presence of external forcing, the most that can be said is the following.

Corollary 2.2. *Solutions to* (1.8) *return infinitely often into a bounded cylinder around the equilibrium manifold*,

$$\liminf_{t\to\infty}\|\mathcal{P}(\boldsymbol{a}-\boldsymbol{c})\|_2 \leq \|\mathcal{P}(\boldsymbol{a})\| < \infty.$$

Proof. Assume, by contradiction, the existence of an $\epsilon > 0$ and a $t_0 > 0$, such that

$$\|\mathcal{P}(\boldsymbol{a} - \boldsymbol{c})\|_2 \geq \|\mathcal{P}(\boldsymbol{a})\|_2 + \epsilon$$

for all $t \geq t_0$, then

$$\frac{\mathrm{d}}{\mathrm{d}t} \int_\Omega \operatorname{tr} \boldsymbol{c} \, \mathrm{d}\boldsymbol{x} \leq -\epsilon$$

for all $t \geq t_0$, which is impossible since this integral is bounded from below. □

The results in this section are based on "algebraic" properties of the system (1.8) and the projection $\mathcal{P}$. These properties yield the conservation of the determinant of $\boldsymbol{c}(\boldsymbol{x})$ and an a-priori estimate for the L^1-like norm

$$\int_\Omega \operatorname{tr} \boldsymbol{c} \, \mathrm{d}\boldsymbol{x} \leq \int_\Omega \operatorname{tr} \boldsymbol{c}_0 \, \mathrm{d}\boldsymbol{x} + \|\mathcal{P}(\boldsymbol{a})\|_2^2 t.$$

Such estimates are not powerful enough for an existence theory, for which L^∞-estimates are needed.

3. A finite-dimensional toy model

The analysis of infinite-dimensional systems is inherently more complex than the analysis of finite-dimensional ones. In this section we construct a finite-dimensional system that retains the algebraic structure of the model problem (1.8), with the hope that the stabilizing mechanism will then be more transparent. We introduce a class of "toy models" in which the evolution takes place in the space $\mathfrak{X}$ of n-vectors of 2-by-2 matrices. An element $\boldsymbol{S} \in \mathfrak{X}$ is a vector with entries S_i, $1 \leq i \leq n$, that are 2-by-2 matrices (we denote their components by $(S_i^{11}, S_i^{12}, S_i^{21}, S_i^{22})$); the time-dependent vector $\boldsymbol{S}(t)$ is analogous to the function $\boldsymbol{c}(\cdot, t)$ in the viscoelastic context. The space $\mathfrak{X}$ is endowed with the inner-product

$$(\boldsymbol{S}, \boldsymbol{R}) = \sum_{i=1}^{n} \operatorname{tr} S_i^{\mathrm{T}} R_i, \tag{3.1}$$

which is the discrete analog of the inner-product (1.9). To simplify notations we introduce the binary operator $\bullet : \mathfrak{X} \times \mathfrak{X} \to \mathfrak{X}$, defined by $(\boldsymbol{R} \bullet \boldsymbol{S})_i = R_i S_i$ (an element-by-element matrix multiplication, also known as a Schur, or Hadamard product). Also, we denote by $\mathfrak{X}_\mathrm{s} \subset \mathfrak{X}$ the subset of vectors whose entries are symmetric matrices, and by $\mathfrak{X}_\mathrm{s}^+ \subset \mathfrak{X}_\mathrm{s}$ the cone of vectors whose entries are symmetric positive-definite matrices.

Let $\mathcal{P} : \mathfrak{X} \to \mathfrak{X}$ be an operator satisfying the following properties: (i) It is a linear operator. (ii) It is symmetric with respect to the inner-product (3.1). (iii) It is a projection, $\mathcal{P} \circ \mathcal{P} = \mathcal{P}$. (iv) Its range consists of vectors of traceless matrices, $\operatorname{tr}[\mathcal{P}(\boldsymbol{S})]_i = 0$. (v) If we define $[\mathcal{P}^{\mathrm{T}}(\boldsymbol{S})]_i = [\mathcal{P}(\boldsymbol{S})]_i^{\mathrm{T}}$, then the ranges of $\mathcal{P}$ and $\mathcal{P}^{\mathrm{T}}$ are orthogonal. This structure imitates the relation between the conformation tensor $\boldsymbol{c}$ and the velocity gradient $\nabla \boldsymbol{u}$. In the next section, we will see how to actually construct linear operators with such properties.

Let $\boldsymbol{A} \in \mathfrak{X}$ be given, and consider the following ordinary differential system in $\mathfrak{X}$,

$$\frac{\mathrm{d}\boldsymbol{S}}{\mathrm{d}t} = \mathcal{P}^{\mathrm{T}}(\boldsymbol{A} - \boldsymbol{S}) \bullet \boldsymbol{S} + \boldsymbol{S} \bullet \mathcal{P}(\boldsymbol{A} - \boldsymbol{S}), \quad \boldsymbol{S}(0) = \boldsymbol{S}_0, \tag{3.2}$$

which is the discrete analog of the model system (1.8). All the results of the previous section apply verbatim to this toy model. In particular, the dynamics (3.2) preserve the determinants $\det S_i$, $1 \leq i \leq n$, symmetric positive-definite initial data give rise to symmetric positive-definite solutions, and the equilibrium manifold

$$\mathcal{M} = \{\boldsymbol{S} \in \mathfrak{X}_\mathrm{s}^+ : \mathcal{P}(\boldsymbol{A} - \boldsymbol{S}) = 0\}$$

contains all equilibrium points in $\mathfrak{X}_\mathrm{s}^+$. Moreover, the growth rate of $\sum_{i=1}^n \operatorname{tr} S_i$ is bounded by a constant, and the ω-limit set of $\|\mathcal{P}(\boldsymbol{A} - \boldsymbol{S})\|_2$ is not empty. System (3.2) defines a $3n$-dimensional polynomial vector field of second degree, which can be reduced into a $2n$-dimensional system by substituting the n invariants $\det S_i$. Note that the control of both the sum of traces and determinants of the S_i implies at once the global existence of solutions. This does not hold in the infinite-dimensional limit, where finite averages do not exclude pointwise blowup.

Unlike in the infinite-dimensional case, we are able to formulate a precise conjecture regarding the long-time asymptotic behavior of solutions.

Conjecture 3.1. *Any solution of system (3.2) with initial data $\boldsymbol{S}_0 \in \mathfrak{X}_\mathrm{s}^+$ converges, as $t \to \infty$, to a fixed point $\boldsymbol{S}^* \in \mathcal{M}$.*

4. Analysis of the toy model

4.1. Explicit representation of $\mathcal{P}$

In this section we analyze the toy model (3.2). We start by fully characterizing the projection operator $\mathcal{P}$, which was introduced through its defining properties. The following properties of $\mathcal{P}$ result from its definition.

Proposition 4.1. *Let $\mathfrak{A} = \operatorname{Range}(\mathcal{P})$, $\mathfrak{B} = \operatorname{Range}(\mathcal{P}^{\mathrm{T}})$, and $\mathfrak{C}$ be the space of element in $\mathfrak{X}$ of the form $\boldsymbol{f} \bullet \boldsymbol{I}$, where $\boldsymbol{f} \in \mathbb{R}^n$, $\boldsymbol{I} \in \mathfrak{X}$ is a vector whose entries are 2-by-2 unit matrices, and $(\boldsymbol{f} \bullet \boldsymbol{I})_i = f_i I$. Then,*

(i) $\mathfrak{A} \cap \mathfrak{B} = \{0\}$.
(ii) $\mathcal{P}(\boldsymbol{R}) = 0$ *for all* $\boldsymbol{R} \in \mathfrak{C}$ (i.e., $\mathfrak{C} \subseteq \ker \mathcal{P}$).
(iii) $\dim \mathfrak{A} = \dim \mathfrak{B} \leq n$.

Proof. The first claim is obvious as any pair of orthogonal subspaces has intersection $\{0\}$.

For every $\boldsymbol{Q} \in \mathfrak{X}$ and $\boldsymbol{f} \in \mathbb{R}^n$,

$$(\mathcal{P}(\boldsymbol{f} \bullet \boldsymbol{I}), \boldsymbol{Q}) = (\boldsymbol{f} \bullet \boldsymbol{I}, \mathcal{P}(\boldsymbol{Q})) = \sum_{i=1}^{n} f_i \operatorname{tr}[\mathcal{P}(\boldsymbol{Q})]_i = 0,$$

i.e., $\mathcal{P}(\boldsymbol{f} \bullet \boldsymbol{I}) = 0$, which proves the second claim.

The ranges of $\mathcal{P}$ and $\mathcal{P}^{\mathrm{T}}$ are obviously isomorphic, thus it remains to show that their dimension cannot be larger than n.

Let $\dim\mathfrak{A} = m$, and consider the space

$$\mathfrak{D} = \{\mathcal{P}(\boldsymbol{S}) - \mathcal{P}^{\mathrm{T}}(\boldsymbol{S}) : \boldsymbol{S} \in \mathfrak{X}\},$$

which is a linear subspace of $\mathfrak{X}$. If $\boldsymbol{U}^1, \ldots, \boldsymbol{U}^m$ is an orthonormal basis for $\mathfrak{A}$, then the m vectors $\mathcal{P}(\boldsymbol{U}^j) - \mathcal{P}^{\mathrm{T}}(\boldsymbol{U}^j)$, $1 \le j \le m$ form an orthogonal set in $\mathfrak{D}$, from which we conclude that $\dim\mathfrak{D} \ge m$. On the other hand, $\mathfrak{D}$ coincides with the subspace of $\mathfrak{X}$ of n-vectors whose elements are traceless anti-symmetric 2-by-2 matrices. Since this subspace if n-dimensional, we conclude that

$$\dim\mathfrak{A} = \dim\mathfrak{B} \le \dim\mathfrak{D} = n. \quad \square$$

We are next going to examine the structure of operators $\mathcal{P}$ satisfying the postulated properties. The projection $\mathcal{P}$ is fully specified by prescribing an orthonormal basis $\{\boldsymbol{U}^1, \ldots, \boldsymbol{U}^n\}$ for its range. Then,

$$\mathcal{P}(\boldsymbol{S}) = \sum_{k=1}^{n} (\boldsymbol{U}^k, \boldsymbol{S})\boldsymbol{U}^k. \tag{4.1}$$

Since each $\boldsymbol{U}^k$ is a vector of traceless matrices, we can write it in the form

$$\boldsymbol{U}^k = \frac{1}{2}\begin{pmatrix} \begin{pmatrix} p_{1k} & a_{1k} \\ b_{1k} & -p_{1k} \end{pmatrix} \\ \vdots \\ \begin{pmatrix} p_{nk} & a_{nk} \\ b_{nk} & -p_{nk} \end{pmatrix} \end{pmatrix}.$$

The condition that the $\boldsymbol{U}^k$ form an orthonormal set gives

$$\frac{1}{4}\sum_{i=1}^{n}(2p_{ik}^2 + a_{ik}^2 + b_{ik}^2) = 1, \quad 1 \le k \le n;$$

$$\frac{1}{4}\sum_{i=1}^{n}(2p_{ij}p_{ik} + a_{ij}a_{ik} + b_{ij}b_{ik}) = 0, \quad 1 \le j < k \le n, \tag{4.2}$$

whereas the condition that the set of $\boldsymbol{U}^j$ be orthogonal to the set of $(\boldsymbol{U}^k)^{\mathrm{T}}$ gives

$$\frac{1}{4}\sum_{i=1}^{n}(2p_{ij}p_{ik} + a_{ij}b_{ik} + b_{ij}a_{ik}) = 0, \quad 1 \le j \le k \le n. \tag{4.3}$$

Subtracting (4.3) from (4.2) we get

$$\frac{1}{4}\sum_{i=1}^{n}(a_{ik} - b_{ik})^2 = 1, \quad 1 \le k \le n;$$

$$\frac{1}{4}\sum_{i=1}^{n}(a_{ij} - b_{ij})(a_{ik} - b_{ik}) = 0, \quad 1 \le j < k \le n. \tag{4.4}$$

This suggests the following change of variables: introduce the n-by-n real-valued matrices $\mathbb{U}$ and $\mathbb{V}$ with entries u_{ij}, v_{ij} defined by

$$u_{ij} := \frac{1}{2}(a_{ij} - b_{ij}), \quad v_{ij} := \frac{1}{2}(a_{ij} + b_{ij}).$$

Then, (4.4) asserts that $\mathbb{U}$ is an orthogonal matrix. At this stage, we can transform the basis $\{\boldsymbol{U}^1, \ldots, \boldsymbol{U}^n\}$ such that the matrix $\mathbb{U}$ becomes a unit matrix.

Rewriting (4.2) and (4.3) in terms of the new parameters we get

$$\sum_{i=1}^{n}(p_{ik}^2 + v_{ik}^2) = 1, \quad 1 \le k \le n;$$

$$\sum_{i=1}^{n}(p_{ij}p_{ik} + v_{ij}v_{ik}) = 0, \quad 1 \le j < k \le n.$$

If we denote by $\mathbb{P}$ the n-by-n real matrix with entries p_{ij}, then the $2n$-by-n matrix $(\mathbb{P}^{\mathrm{T}}, \mathbb{V}^{\mathrm{T}})^{\mathrm{T}}$ is orthogonal. We have thus shown that the defining properties of the projection $\mathcal{P}$ amount to the following characterization.

Proposition 4.2. *The range of $\mathcal{P}$ is spanned by an orthonormal basis $\{\boldsymbol{U}^1, \ldots, \boldsymbol{U}^n\}$, where each $\boldsymbol{U}^k$ is of the form*

$$\boldsymbol{U}^k = \frac{1}{2}\begin{pmatrix} \begin{pmatrix} p_{1k} & v_{1k} + \delta_{1k} \\ v_{1k} - \delta_{1k} & -p_{1k} \end{pmatrix} \\ \vdots \\ \begin{pmatrix} p_{nk} & v_{nk} + \delta_{nk} \\ v_{nk} - \delta_{nk} & -p_{nk} \end{pmatrix} \end{pmatrix}, \tag{4.5}$$

where δ_{ij} is Kronecker's delta, and the parameters p_{ij}, v_{ij} are the respective entries of n-by-n matrices $\mathbb{P}$, $\mathbb{V}$, such that the $2n$-by-n matrix $(\mathbb{P}^{\mathrm{T}}, \mathbb{V}^{\mathrm{T}})^{\mathrm{T}}$ is orthogonal.

4.2. Change of variables

In this subsection we take advantage of the explicit characterization of $\mathcal{P}$ to simplify the structure of the dynamical system (3.2). Substituting the representation (4.1) of the projection into (3.2) the differential system takes the form

$$\frac{\mathrm{d}\boldsymbol{S}}{\mathrm{d}t} = \sum_{k=1}^{n}(a_k - y_k)[(\boldsymbol{U}^k)^{\mathrm{T}} \bullet \boldsymbol{S} + \boldsymbol{S} \bullet \boldsymbol{U}^k], \tag{4.6}$$

where the real-valued n-vectors $\boldsymbol{y}, \boldsymbol{a}$ with entries y_k and a_k are defined by

$$y_k := (\boldsymbol{S}, \boldsymbol{U}^k), \quad a_k := (\boldsymbol{A}, \boldsymbol{U}^k). \tag{4.7}$$

We will now rewrite this $3n$-dimensional system as a system for three n-vectors $\boldsymbol{x}, \boldsymbol{r}, \boldsymbol{s}$, whose components are defined by

$$x_i := \frac{1}{2}(S_i^{11} + S_i^{22}), \quad r_i := \frac{1}{2}(S_i^{11} - S_i^{22}), \quad s_i := S_i^{12}.$$

The conservation of the determinants and the positive-definiteness of the matrices S_i imply that each of the x_i is positive and that

$$\beta_i := x_i^2 - r_i^2 - s_i^2$$

are positive integrals of motion.

Substituting the explicit representation (4.5) of the basis vectors $\boldsymbol{U}^k$ into (4.7), the vector $\boldsymbol{y}$ reduces to

$$\boldsymbol{y} = \mathbb{P}^{\mathrm{T}}\boldsymbol{r} + \mathbb{V}^{\mathrm{T}}\boldsymbol{s}. \tag{4.8}$$

By a straightforward substitution, the vectors $\boldsymbol{x}$, $\boldsymbol{r}$, $\boldsymbol{s}$ are found to satisfy the differential system:

$$\begin{aligned}
\frac{\mathrm{d}\boldsymbol{x}}{\mathrm{d}t} &= [\mathbb{P}(\boldsymbol{a}-\boldsymbol{y})] \bullet \boldsymbol{r} + [\mathbb{V}(\boldsymbol{a}-\boldsymbol{y})] \bullet \boldsymbol{s},\\
\frac{\mathrm{d}\boldsymbol{r}}{\mathrm{d}t} &= [\mathbb{P}(\boldsymbol{a}-\boldsymbol{y})] \bullet \boldsymbol{x} - (\boldsymbol{a}-\boldsymbol{y}) \bullet \boldsymbol{s},\\
\frac{\mathrm{d}\boldsymbol{s}}{\mathrm{d}t} &= (\boldsymbol{a}-\boldsymbol{y}) \bullet \boldsymbol{r} + [\mathbb{V}(\boldsymbol{a}-\boldsymbol{y})] \bullet \boldsymbol{x},
\end{aligned} \tag{4.9}$$

where here $\bullet : \mathbb{R}^n \times \mathbb{R}^n \to \mathbb{R}^n$ stands for a term-by-term multiplication of n-vectors.

The differential system (4.9) with $\boldsymbol{y}$ given by (4.8) provides an alternative representation of our original system (3.2). It is a $3n$-dimensional system with n invariants β_i, and can easily be reduced into a $2n$-dimensional system by viewing the β_i as given (positive) parameters, and setting

$$x_i = \sqrt{\beta_i + r_i^2 + s_i^2}.$$

In particular, the equilibrium set of this system is the hyper-plane $\boldsymbol{y} = \boldsymbol{a}$.

Since the vector $\boldsymbol{y}$ plays such a distinguished role, it is useful to transform the system (4.9) once more, into a parametrization where $\boldsymbol{y}$ is one of the variables. For that, we introduce n-by-n matrices $\mathbb{Q}$ and $\mathbb{W}$, with entries q_{ij}, w_{ij}, which complement the matrices $\mathbb{P}$, $\mathbb{V}$, such that the linear transformation

$$\begin{pmatrix} \boldsymbol{y} \\ \boldsymbol{z} \end{pmatrix} := \begin{pmatrix} \mathbb{P}^{\mathrm{T}} & \mathbb{V}^{\mathrm{T}} \\ \mathbb{Q}^{\mathrm{T}} & \mathbb{W}^{\mathrm{T}} \end{pmatrix} \begin{pmatrix} \boldsymbol{r} \\ \boldsymbol{s} \end{pmatrix}$$

is orthogonal. Eliminating $\boldsymbol{r}$ and $\boldsymbol{s}$ we see that the vectors $\boldsymbol{x}$, $\boldsymbol{y}$, $\boldsymbol{z}$ satisfy the system

$$\begin{aligned}
\frac{\mathrm{d}\boldsymbol{x}}{\mathrm{d}t} &= [\mathbb{P}(\boldsymbol{a}-\boldsymbol{y})] \bullet (\mathbb{P}\boldsymbol{y} + \mathbb{Q}\boldsymbol{z}) + [\mathbb{V}(\boldsymbol{a}-\boldsymbol{y})] \bullet (\mathbb{V}\boldsymbol{y} + \mathbb{W}\boldsymbol{z}),\\
\frac{\mathrm{d}\boldsymbol{y}}{\mathrm{d}t} &= \mathbb{P}^{\mathrm{T}}\{[\mathbb{P}(\boldsymbol{a}-\boldsymbol{y})] \bullet \boldsymbol{x} - (\boldsymbol{a}-\boldsymbol{y}) \bullet (\mathbb{V}\boldsymbol{y} + \mathbb{W}\boldsymbol{z})\}\\
&\quad + \mathbb{V}^{\mathrm{T}}\{[\mathbb{V}(\boldsymbol{a}-\boldsymbol{y})] \bullet \boldsymbol{x} + (\boldsymbol{a}-\boldsymbol{y}) \bullet (\mathbb{P}\boldsymbol{y} + \mathbb{Q}\boldsymbol{z})\},\\
\frac{\mathrm{d}\boldsymbol{z}}{\mathrm{d}t} &= \mathbb{Q}^{\mathrm{T}}\{[\mathbb{P}(\boldsymbol{a}-\boldsymbol{y})] \bullet \boldsymbol{x} - (\boldsymbol{a}-\boldsymbol{y}) \bullet (\mathbb{V}\boldsymbol{y} + \mathbb{W}\boldsymbol{z})\}\\
&\quad + \mathbb{W}^{\mathrm{T}}\{[\mathbb{V}(\boldsymbol{a}-\boldsymbol{y})] \bullet \boldsymbol{x} + (\boldsymbol{a}-\boldsymbol{y}) \bullet (\mathbb{P}\boldsymbol{y} + \mathbb{Q}\boldsymbol{z})\}.
\end{aligned}$$

This system can be recast in simpler typographical form by introducing a ternary product on n-by-n matrices,

$$\langle \mathbb{A}, \mathbb{B}, \mathbb{C} \rangle_{ijk} := \sum_{m=1}^{n} a_{mi} b_{mj} c_{mk},$$

and noting the following identities,

$$[(\mathbb{A}\boldsymbol{x}) \bullet (\mathbb{B}\boldsymbol{y})]_i = \sum_{j,k=1}^{n} \langle \mathbb{I}, \mathbb{A}, \mathbb{B} \rangle_{ijk} x_j y_k,$$

$$[\mathbb{A}^{\mathrm{T}}\{(\mathbb{B}\boldsymbol{x}) \bullet \boldsymbol{y}\}]_i = \sum_{j,k=1}^{n} \langle \mathbb{A}, \mathbb{B}, \mathbb{I} \rangle_{ijk} x_j y_k.$$

Then,

$$\frac{\mathrm{d}}{\mathrm{d}t}\begin{pmatrix} x_i \\ y_i \\ z_i \end{pmatrix} = \sum_{j,k=1}^{n} (a_j - y_j) M_{ijk} \begin{pmatrix} x_k \\ y_k \\ z_k \end{pmatrix}, \tag{4.10}$$

where the M_{ijk} are 3-by-3 matrices given by

$$M_{ijk} := \begin{pmatrix} 0 & \langle \mathbb{I}, \mathbb{P}, \mathbb{P} \rangle + \langle \mathbb{I}, \mathbb{V}, \mathbb{V} \rangle & \langle \mathbb{I}, \mathbb{P}, \mathbb{Q} \rangle + \langle \mathbb{I}, \mathbb{V}, \mathbb{W} \rangle \\ \langle \mathbb{P}, \mathbb{P}, \mathbb{I} \rangle + \langle \mathbb{V}, \mathbb{V}, \mathbb{I} \rangle & \langle \mathbb{V}, \mathbb{I}, \mathbb{P} \rangle - \langle \mathbb{P}, \mathbb{I}, \mathbb{V} \rangle & \langle \mathbb{V}, \mathbb{I}, \mathbb{Q} \rangle - \langle \mathbb{P}, \mathbb{I}, \mathbb{W} \rangle \\ \langle \mathbb{Q}, \mathbb{P}, \mathbb{I} \rangle + \langle \mathbb{W}, \mathbb{V}, \mathbb{I} \rangle & \langle \mathbb{W}, \mathbb{I}, \mathbb{P} \rangle - \langle \mathbb{Q}, \mathbb{I}, \mathbb{V} \rangle & \langle \mathbb{W}, \mathbb{I}, \mathbb{Q} \rangle - \langle \mathbb{Q}, \mathbb{I}, \mathbb{W} \rangle \end{pmatrix}_{ijk}.$$

In terms of the new variables, the integrals of motion are

$$\beta_i = x_i^2 - (\mathbb{P}\boldsymbol{y} + \mathbb{Q}\boldsymbol{z})_i^2 - (\mathbb{V}\boldsymbol{y} + \mathbb{W}\boldsymbol{z})_i^2.$$

4.3. Local stability of the equilibrium manifold

All point on the hyper-plane $\boldsymbol{y} = \boldsymbol{a}$ are equilibria (and are the only equilibria when the integrals of motion β_i are positive). To analyze the linear stability of these equilibria we consider a perturbation,

$$\boldsymbol{y}(t) = \boldsymbol{a} + \delta\boldsymbol{y}(t), \quad \boldsymbol{z}(t) = \hat{\boldsymbol{z}} + \delta\boldsymbol{z}(t),$$

and linearize system (4.10) about the perturbations. The linearized system has an n-dimensional neutral manifold which coincides with the equilibrium hyper-plane. In the n-dimensional space that is perpendicular to the equilibrium hyper-plane the linear system takes the form

$$\frac{\mathrm{d}}{\mathrm{d}t}\delta\boldsymbol{y} = -\mathbb{C}\,\delta\boldsymbol{y},$$

where the n-by-n matrix $\mathbb{C}$ has entries

$$\begin{aligned}
c_{ij} &= \sum_{k=1}^{n} (\langle \mathbb{P}, \mathbb{P}, \mathbb{I} \rangle + \langle \mathbb{V}, \mathbb{V}, \mathbb{I} \rangle)_{ijk} x_k\\
&\quad + \sum_{k=1}^{n} (\langle \mathbb{V}, \mathbb{I}, \mathbb{P} \rangle - \langle \mathbb{P}, \mathbb{I}, \mathbb{V} \rangle)_{ijk} a_k\\
&\quad + \sum_{k=1}^{n} (\langle \mathbb{V}, \mathbb{I}, \mathbb{Q} \rangle - \langle \mathbb{P}, \mathbb{I}, \mathbb{W} \rangle)_{ijk} \hat{z}_k,
\end{aligned}$$

where here

$$x_k = \sqrt{\beta_k + (\mathbb{P}\boldsymbol{a} + \mathbb{Q}\hat{\boldsymbol{z}})_k^2 + (\mathbb{V}\boldsymbol{a} + \mathbb{W}\hat{\boldsymbol{z}})_k^2}.$$

An equilibrium point is linearly stable if and only if all the eigenvalues of $\mathbb{C}$ are positive. The example studied in the next section shows that equilibria may be linearly unstable, i.e., the equilibrium manifold may be partitioned into linearly stable and linearly unstable domains. The only general statement that can be made about the linearized dynamics is the following.

Proposition 4.3. *The trace of the matrix $\mathbb{C}$ is positive, i.e., the dynamics in the vicinity of the equilibrium hyper-plane are volume contracting.*

Proof. An explicit summation gives

$$\operatorname{tr}\mathbb{C} = \sum_{i=1}^{n} [x_i + v_{ii}(\mathbb{P}\boldsymbol{a} + \mathbb{Q}\hat{\boldsymbol{z}})_i - p_{ii}(\mathbb{V}\boldsymbol{a} + \mathbb{W}\hat{\boldsymbol{z}})_i].$$

Since the columns of the matrix $[\mathbb{P}^{\mathrm{T}}, \mathbb{V}^{\mathrm{T}}]^{\mathrm{T}}$ are orthonormal, it follows that $v_{ii}^2 + p_{ii}^2 \le 1$ and by the Cauchy–Schwarz inequality,

$$|v_{ii}(\mathbb{P}\boldsymbol{a} + \mathbb{Q}\hat{\boldsymbol{z}})_i - p_{ii}(\mathbb{V}\boldsymbol{a} + \mathbb{W}\hat{\boldsymbol{z}})_i| \le \sqrt{(\mathbb{P}\boldsymbol{a} + \mathbb{Q}\hat{\boldsymbol{z}})_i^2 + (\mathbb{V}\boldsymbol{a} + \mathbb{W}\hat{\boldsymbol{z}})_i^2},$$

hence

$$\operatorname{tr}\mathbb{C} \ge \sum_{i=1}^{n} \left[x_i - \sqrt{(\mathbb{P}\boldsymbol{a} + \mathbb{Q}\hat{\boldsymbol{z}})_i^2 + (\mathbb{V}\boldsymbol{a} + \mathbb{W}\hat{\boldsymbol{z}})_i^2} \right] \ge 0,$$

where we have used the fact that

$$x_i^2 = \beta_i + (\mathbb{P}\boldsymbol{a} + \mathbb{Q}\hat{\boldsymbol{z}})_i^2 + (\mathbb{V}\boldsymbol{a} + \mathbb{W}\hat{\boldsymbol{z}})_i^2 > (\mathbb{P}\boldsymbol{a} + \mathbb{Q}\hat{\boldsymbol{z}})_i^2 + (\mathbb{V}\boldsymbol{a} + \mathbb{W}\hat{\boldsymbol{z}})_i^2. \quad \square$$

5. An example

The lowest-dimensional systems for which one gets non-trivial dynamics are for $n = 2$. That is, a six-dimensional system which can be further reduced to four dimensions by substituting the invariants of motion. Such a system is determined by the 2-by-2 matrices $\mathbb{P}$, $\mathbb{V}$, and "forcing" vector $\boldsymbol{a}$.

Consider the choice

$$\mathbb{P} = \frac{1}{\sqrt{2}}\begin{pmatrix} 0 & 1 \\ 0 & 1 \end{pmatrix}, \quad \mathbb{V} = \frac{1}{\sqrt{2}}\begin{pmatrix} 1 & 0 \\ -1 & 0 \end{pmatrix},$$

which we complement taking

$$\mathbb{Q} = \frac{1}{\sqrt{2}}\begin{pmatrix} 0 & 1 \\ 0 & -1 \end{pmatrix}, \quad \mathbb{W} = \frac{1}{\sqrt{2}}\begin{pmatrix} 1 & 0 \\ 1 & 0 \end{pmatrix}.$$

Substituting into (4.10), it is a matter of tedious, yet, straightforward algebra to derive the following quadratic system in $\mathbb{R}^6$,

$$\frac{\mathrm{d}}{\mathrm{d}t}\begin{pmatrix} x_1 \\ y_1 \\ z_1 \\ x_2 \\ y_2 \\ z_2 \end{pmatrix} = \frac{1}{2}(a_1 - y_1)\begin{pmatrix} 0 & 1 & 1 & 0 & 0 & 0 \\ 1 & 0 & 0 & 1 & 1 & 1 \\ 1 & 0 & 0 & -1 & 1 & 1 \\ 0 & 1 & -1 & 0 & 0 & 0 \\ 0 & -1 & -1 & 0 & 0 & 0 \\ 0 & -1 & -1 & 0 & 0 & 0 \end{pmatrix}\begin{pmatrix} x_1 \\ y_1 \\ z_1 \\ x_2 \\ y_2 \\ z_2 \end{pmatrix} + \frac{1}{2}(a_2 - y_2)\begin{pmatrix} 0 & 0 & 0 & 0 & 1 & 1 \\ 0 & 0 & 0 & 0 & -1 & 1 \\ 0 & 0 & 0 & 0 & 1 & -1 \\ 0 & 0 & 0 & 0 & 1 & -1 \\ 1 & 1 & -1 & 1 & 0 & 0 \\ 1 & -1 & 1 & -1 & 0 & 0 \end{pmatrix}\begin{pmatrix} x_1 \\ y_1 \\ z_1 \\ x_2 \\ y_2 \\ z_2 \end{pmatrix}. \tag{5.1}$$

The two invariants of motion are

$$\beta_1 = x_1^2 - \frac{1}{2}(y_2 + z_2)^2 - \frac{1}{2}(y_1 + z_1)^2,$$

$$\beta_2 = x_2^2 - \frac{1}{2}(y_2 - z_2)^2 - \frac{1}{2}(y_1 - z_1)^2.$$

We start by checking under what conditions is the equilibrium plane $\boldsymbol{y} = \boldsymbol{a}$ linearly stable. Throughout this example, we take $\beta_1 = \beta_2 = 1$, so that the vector $\boldsymbol{x}$ is determined by the vectors $\boldsymbol{y}, \boldsymbol{z}$, and we consider the above system as four-dimensional. Consider then a perturbation about an equilibrium point,

$$\boldsymbol{y}(t) = \boldsymbol{a} + \delta\boldsymbol{y}(t), \quad \boldsymbol{z}(t) = \hat{\boldsymbol{z}} + \delta\boldsymbol{z}(t).$$

Substituting and linearizing about the fixed point $\boldsymbol{y} = \boldsymbol{a}$, $\boldsymbol{z} = \hat{\boldsymbol{z}}$, we obtain the linear system

$$\frac{\mathrm{d}}{\mathrm{d}t}\begin{pmatrix} \delta y_1 \\ \delta y_2 \\ \delta z_1 \\ \delta z_2 \end{pmatrix} = -\frac{1}{2}\begin{pmatrix} x_1 + x_2 + a_2 + \hat{z}_2 & \hat{z}_2 - a_2 & 0 & 0 \\ -a_1 - \hat{z}_1 & x_1 + x_2 + a_1 - \hat{z}_1 & 0 & 0 \\ x_1 - x_2 + a_2 + \hat{z}_2 & a_2 - \hat{z}_2 & 0 & 0 \\ -a_1 - \hat{z}_1 & x_1 - x_2 - a_1 + \hat{z}_1 & 0 & 0 \end{pmatrix} \times \begin{pmatrix} \delta y_1 \\ \delta y_2 \\ \delta z_1 \\ \delta z_2 \end{pmatrix},$$

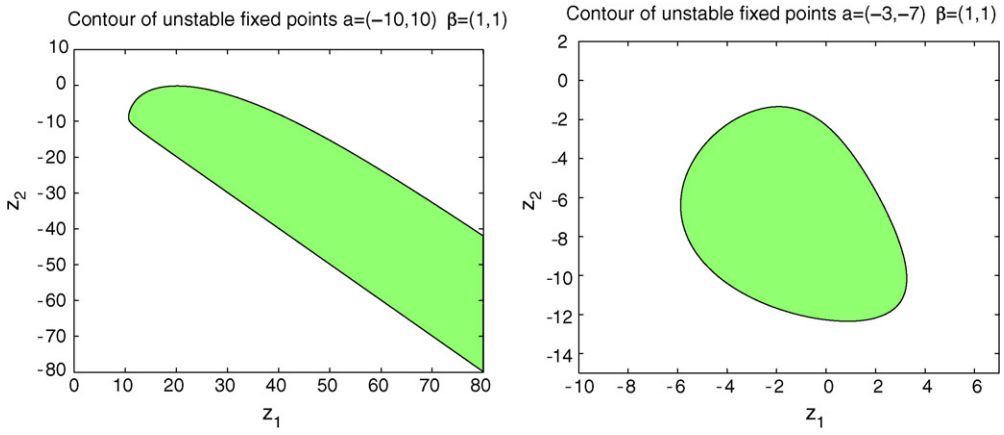

Fig. 3. Region of unstable equilibria on the $\hat{z}$-plane for $\boldsymbol{a} = (-10, 10)$ (left) and $\boldsymbol{a} = (-3, -7)$ (right).

with the vector $\boldsymbol{x}$ given by

$$x_1 = \sqrt{\beta_1 + \frac{1}{2}(a_2 + \hat{z}_2)^2 + \frac{1}{2}(a_1 + \hat{z}_1)^2},$$

$$x_2 = \sqrt{\beta_2 + \frac{1}{2}(a_2 - \hat{z}_2)^2 + \frac{1}{2}(a_1 - \hat{z}_1)^2}.$$

As expected, this system has two neutral directions that lie on the equilibrium plane, so that linear stability is determined by considering the restriction of this system to the $\boldsymbol{y}$-plane. The trace of this 2-by-2 matrix equals

$$-\left[x_1 + \frac{1}{2}(a_1 - \hat{z}_1) + x_2 + \frac{1}{2}(a_2 + \hat{z}_2)\right],$$

which is always negative. The fixed point is stable then if the determinant of this matrix is positive, i.e., when

$$(x_1 + x_2 + a_2 + \hat{z}_2)(x_1 + x_2 + a_1 - \hat{z}_1) + (a_1 + \hat{z}_1)(\hat{z}_2 - a_2) > 0.$$

It turns out that the equilibrium plane can have sets that are unstable. For fixed values of the vectors $\boldsymbol{a}$ and $\boldsymbol{\beta}$, the boundary of the unstable equilibria are curves on the $\hat{z}$ plane.

In Fig. 3 we plot in shaded color sets of unstable equilibria on the $\hat{z}$ plane for $\boldsymbol{a} = (-10, 10)$ (left) and $\boldsymbol{a} = (-3, -7)$ (right). In the first case the domain of unstable equilibria is unbounded, whereas in the second case it is compact.

The presence of unstable equilibria may shed doubt on the validity of Conjecture 3.1. However, numerical solutions that start in the vicinity of unstable fixed points indicate that after a transient of exponential repulsion from the equilibrium manifold, all trajectories converge back toward a (stable) equilibrium. This situation is depicted in Fig. 4 where we show the evolution of $\boldsymbol{y}(t) - \boldsymbol{a}$ (i.e., the displacement from the equilibrium manifold) for a trajectory that starts in the vicinity of an unstable equilibrium. Note the long transient and the "spiking" behavior of the Euclidean distance of the solution from the equilibrium manifold.

Although we cannot provide a proof, our calculations indicate that all solutions starting in the vicinity of the unstable equilibria, e.g., for the parameters depicted in Fig. 3(right), reach stable equilibria on the same plane. A trajectory that connects two different fixed points is known as a heteroclinic orbit. In the present example, since the unstable manifold at an unstable fixed point is one dimensional (by Proposition 4.3), there are two heteroclinic orbits, going in opposite directions, for each unstable point. These orbits define a mapping between points on the equilibrium plane: every linearly unstable point on that plane is mapped into a pair of points, that are linearly stable. This mapping can be extended to the whole equilibrium plane in a natural way: a stable point is mapped into itself. Thus, we have defined a bi-valued mapping, which we call the heteroclinic map, from the equilibrium plane into itself. Note that this mapping is in general not continuous at the boundary of the unstable set; indeed, the dependence on initial data is only continuous for finite time. Therefore one cannot apply topological considerations, such as homotopy theory.

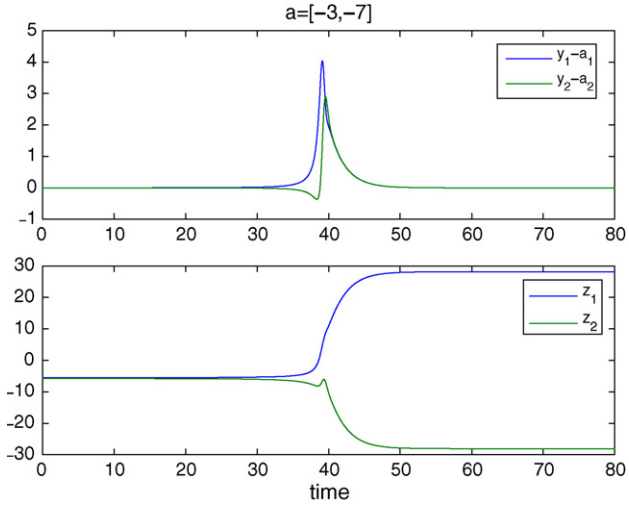

Fig. 4. Evolution of the vector $\boldsymbol{y}(t) - \boldsymbol{a}$ (top) and $\boldsymbol{z}(t)$ (bottom) for the parameters $\boldsymbol{a} = (-3, -7)$ and initial data in the vicinity of the equilibrium point $\boldsymbol{y} = \boldsymbol{a}$ and $\boldsymbol{z} = (-5.5, -5.5)$.

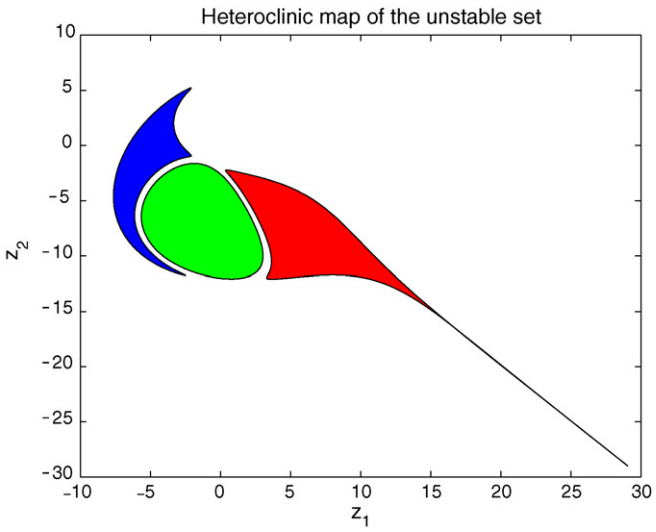

Fig. 5. The heteroclinic map for the parameters used in Fig. 3(left). Every point in the green region – the domain of unstable points – is mapped into two points in the stable set. The red and blue areas are the images of the green area under the heteroclinic map. (For interpretation of the references to color in this figure legend, the reader is referred to the web version of the article.)

In Fig. 5 we display the heteroclinic map for a set of points along the boundaries of the sets of unstable equilibria shown in Fig. 3(right). That is, for every such point we display the two points at the ends of the orbits that emanate from it. Every point on the unstable side of the boundary has one heteroclinic orbit whose end is on the stable side of the boundary (i.e., this branch of the heteroclinic map is continuous), and one heteroclinic orbit that lands on the equilibrium plane at a distant point; this branch of the heteroclinic map is discontinuous as the initial point crosses the boundary of the unstable set. The green area corresponds to the unstable set, whereas the blue and red areas are its image under the bi-valued heteroclinic map. Each of the two images has a joint boundary with the unstable set, indicating the continuity of the heteroclinic map along part of the boundary of the unstable set. Note, in addition, the strong cusp in the right branch of the heteroclinic mapping. We checked for the possibility that this cusp is indicative of a critical trajectory that diverges asymptotically, but careful computations indicate that this cusp is finite.

6. Conclusions

We have presented here a partial analysis complemented with numerical results of model systems inspired by the Oldroyd-B model in the creeping flow regime. Our primary motivation in the development of these models was to capture the nonlinear coupling between the stretching of the conformation tensor and stress-induced velocity field. Our working hypothesis was that a well-posed system must exhibit a negative feedback, where the stress field generates a flow field that represses its originating source. In Section 2 we analyzed a system derived from the Oldroyd-B model, in which the stress-advection and stress-relaxation have been discarded. Although we have not been able to prove it, numerical experiments indicate that such a system always tends to a static equilibrium, even if this involves the formation of highly singular stress fields. It should be pointed out, however, that our analysis is only valid for models that have non-zero solvent viscosity, and does not apply, for example, to the upper-convected Maxwell model. Moreover, we restrict ourselves to shearing and forcing boundary conditions, but our analysis does not apply to flow geometries with imposed inflows.

In the succeeding sections we presented and analyzed a finite-dimensional toy model that has the same algebraic structure as the infinite-dimensional system of Section 2. Here again, simulations indicate that such systems always tends asymptotically in time to an equilibrium, but all our attempts to prove this conjecture have failed. An examination of a particular four-dimensional system reveals a surprisingly rich behavior, where the equilibrium manifold may exhibit regions of stable and unstable equilibria connected by heteroclinic trajectories. Thus, a system may start arbitrarily close to an equilibrium, be repelled away from the equilibrium manifold (a "spiking" behavior), before ending back on the manifold at a point which may be distant from the starting point.

While we have proved that solutions to the infinite-dimensional system (1.8) (a forteriori, the finite-dimensional system (3.2)) cannot wander far away from the equilibrium manifold for too long, we were not able to prove that these solutions remain bounded. Moreover, it is conceivable that the system tends asymptotically to the equilibrium manifold without converging to a specific point on that manifold. The equilibrium manifold consists of stress fields satisfying $\operatorname{div} \boldsymbol{c} = \operatorname{div} \boldsymbol{a}$. Thus, convergence to the equilibrium manifold may well be accompanied with the formation of singular structures that have zero divergence. Such a scenario comes in mind in light of the recently discovered role of singular divergence-free stress fields in the linear stability of Couette flow [9].

One of the goals stated in Section 1 was to draw practical implications for numerical methods. The obvious implication is the necessity of preserving the positive-definiteness of the conformation tensor. Indeed, the loss of positive-definiteness, even at a single point, can have deleterious consequences, notably blowup. This conclusion is consistent with a longstanding experience, where the loss of positivity was observed as a precursor of blowup. Moreover, methods that impose positive-definiteness, such as the stochastic method of Brownian configuration fields, are known to exhibit improved stability.

One aspect of the dynamics which was not addressed in this paper is the sensitivity of the stable behavior on the precise structure of the model. As a test, we perturbed the case study (5.1) by adding small (of the order of 10^{-3}) perturbations to the matrix elements. Such perturbations completely destroyed the nature of the equations, causing in many cases solutions to diverge in time. This means that it is crucial for numerical discretizations to correctly retain the algebraic properties of the differential operators. In particular, the discrete projection operator that converts stress fields into velocity gradients, must be symmetric and positive. High-order methods, for example, methods that use nonlinear flux limiters, often reduce truncation errors on the expense of the algebraic structure.

In this respect, the numerical solutions shown in Section 2 are disappointing. While these results are not intended to capture any physical reality, they are instructive. By carefully choosing a discretization that preserves the essential algebraic properties of the differential operators we produced solutions that, for any given mesh, tend to a stable equilibrium, even when singular boundary conditions are imposed. Yet, this stability does not prevent the stress profile to become increasingly singular as the mesh is refined. This indicates that the stabilizing mechanism does not prevent the formation of singularities. This should not be of a surprise, given that the projection operator $\mathcal{P}$ has an infinite-dimensional kernel consisting of all divergence-free stress fields. The set of divergence-free stress fields includes singular functions, and even distribution-valued (generalized) functions. This observation raises once again the question whether models of Oldroyd-type do not miss a crucial ingredient of spatial coupling, for example, stress diffusion (a discussion of this issue can be found in [10,9]).

In a sense, this paper raises more questions than it solves. Its interest, we believe, is in the revelation of new aspects of the stress–flow coupling in viscoelastic models. Moreover, we believe that a proof of our main conjecture may pave the way toward an existence theory for the Oldroyd-B model in the creeping flow regime. The essential stumblingblock in the development of an existence theory is to control the growth of the stress field. Since the equations of motion are quadratic in the stress, there is a danger of finite-time blowup. Clearly, to exclude such a scenario, a new control mechanism has to be revealed. We believe that, if it exists, such a mechanism has to be inherent in the structure of the stress–velocity coupling.

As a final comment, we note that we have nowhere used the fact that the matrices were 2-by-2. Preliminary results indicate that our global stability conjecture remains valid for vectors whose entries are arbitrary d-by-d matrices, as long as the algebraic structure remains the same.

Acknowledgments

We are grateful to Emmanuel Farjoun, Haim Sompolinsky, Edriss Titi and Benjamin Weiss for helpful advice. We also thank the anonymous reviewers for their very useful comments. RK was partially supported by the Israel Science Foundation founded by the Israel Academy of Sciences and Humanities. RF was supported by the Miller Foundation. GK was partially supported by the Edmund Landau Center for Research in Mathematical Analysis and Related Areas, sponsored by the Minerva Foundation (Germany).

References

[1] R.B. Bird, R.C. Armstrong, O. Hassager, Dynamics of Polymeric Liquids, vol. 1, John Wiley and Sons, New York, 1987.
[2] R.G. Larson, Constitutive Equations for Polymer Melts and Solutions. Butterworths Series in Chemical Engineering, 1988.
[3] R. Fattal, R. Kupferman, Constitutive laws for the matrix-logarithm of the conformation tensor, J. Non-Newton. Fluid Mech. 123 (2004) 281–285.
[4] R. Fattal, R. Kupferman, Time-dependent simulation of viscoelastic flows at high Weissenberg number using the log-conformation representation, J. Non-Newton. Fluid Mech. 126 (2005) 23–37.
[5] M.A. Hulsen, R. Fattal, R. Kupferman, Flow of viscoelastic fluids past a cylinder at high Weissenberg number: stabilized simulations using matrix logarithms, J. Non-Newton. Fluid Mech. 127 (2005) 27–39.
[6] T.N. Phillips, A.J. Williams, Comparison of creeping and inertial flow of an Oldroyd B fluid through planar and axisymmetric contractions, J. Non-Newton. Fluid Mech. 108 (2002) 25–47.
[7] M.A. Hulsen, A.P.G. van Heel, B.H.A.A. van den Brule, Simulation of viscoelastic flows using brownian configuration fields, J. Non-Newton. Fluid. Mech. 70 (1997) 79–101.
[8] G. Katriel, R. Kupferman, E.S. Titi. Global existence and long-time limit for a class of nonlinear infinite-dimensional dynamical systems, in preparation.
[9] R. Kupferman, On the linear stability of plane Couette flow for an Oldroyd-B fluid and its numerical approximation, J. Non-Newton. Fluid Mech. 127 (2005) 169–190.
[10] A.W. El-Kareh, L.G. Leal, Existence of solutions for all Deborah numbers for a non-Newtonian model modified to include diffusion, J. Non-Newton. Fluid Mech. 33 (1989) 257–287.